Physicochemical Characterization of Natural Ionic Microreservoirs: Bacillus subtilis Dormant Spores

ARTICLE *in* THE JOURNAL OF PHYSICAL CHEMISTRY B · MARCH 2008

Impact Factor: 3.3 · DOI: 10.1021/jp077188u · Source: PubMed

3 AUTHORS, INCLUDING:

Sergey Kazakov
Pace University
47 PUBLICATIONS **436** CITATIONS
SEE PROFILE

Irina G Gazaryan
Burke Medical Research Institute New York
89 PUBLICATIONS **2,347** CITATIONS
SEE PROFILE

Physicochemical Characterization of Natural Ionic Microreservoirs: *Bacillus subtilis* Dormant Spores

Sergey Kazakov,*,† Elizabeth Bonvouloir,† and Irina Gazaryan‡

Department of Chemistry and Physical Sciences, Pace University, 861 Bedford Road, Pleasantville, New York 10570, and Burke Medical Research Institute, 785 Mamaroneck Avenue, White Plains, New York 10605

Received: September 6, 2007; In Final Form: December 4, 2007

The kinetics of proton exchange between dormant spores and aqueous environment was examined by time-resolved micropotentiometry, the method we recently introduced for hydrogel particles of micro- and nanometer diameter (*J. Phys. Chem. B* **2006**, *110,* 15107). In this work, the method was applied to the suspensions of dormant *Bacillus subtilis* spore of different concentrations to show that proton uptake kinetics was a multistep process involving a number of successively ∼10-fold slower steps of proton penetration into the bulk and their binding to the ionizable groups within different layers of a spore structure. By analyzing the proton equilibrium binding to ionizable groups inside a spore, it was shown that each *Bacillus subtilis* spore behaves like almost infinite ionic reservoir capable of accumulating billions of protons ($N \sim 2 \times 10^{10}$ per spore). The obtained pK_a value of 4.7 for the spores studied is the first quantitative indication on carboxyl groups as the major ionizable groups fixed in a spore matrix. In general, proton equilibrium binding within the spore matrix obeys the fundamental law of the Langmuir isotherm. The proton binding to the ionizable groups slows down the free proton diffusion within a spore, but this effect is substantially weakened by increasing the initial concentration of protons added. On the basis of the diffusion time analysis, it was found that the effective diffusion coefficient for hydrogen ions within the spore core can be up to 3 orders of magnitude lower than that within the coats and cortex. We speculate that the spore inner membrane which separates core from cortex and coats in a dormant spore is a major permeability barrier for protons to penetrate into a lockbox of the genetic information (core).

Introduction

Considerable attention has been paid to the ionic exchange in bulk hydrogels, hydrogel submicro- and nanospheres, and polyelectrolyte microcapsules.[1−11] By now, it is well-established that charged groups attached to the polymer chains play an essential role in the ionic sensitivity of the polymer networks. Examining the interactions between *Bacillus subtilis* spores and specifically modified liposomes,[12] we suggested that the dormant spores of bacteria are naturally occurred microcapsules which could behave like ionic hydrogels capable of uptaking and releasing ions.

A bacterial spore is a single cell, in which the genetic information is enclosed into the spore core surrounded by two types of walls, an inner-peptidoglycan-wall (spore cortex), and an outer-protein-wall (spore coats). A dormant spore has to be environmentally resistant[13−15] in order to protect the locked genome. "Dormant life" supposes the shutdown of metabolic activity, that is, macromolecular synthesis and exchange of large molecules. Despite numerous microbiological and biochemical studies [refs 13−20 and references therein] undertaken to reveal the crucial biochemical reactions and drastic physical transformations at all three steps of spore germination (activation, commitment, and vegetative outgrowth), the chain of molecular mechanisms operating in a dormant spore is still not understood. It is not clear how spores intrinsically respond to the changes in the external conditions (temperature, concentration of ions, etc.). We believe that if a metabolically inactive spore is not capable of exchanging large molecules with the environment, the ions might be the principle agents involved in the spore sensory mechanism in the dormant state.

It is well-documented that ions play an important role in activation of spore germination.[15,21−25] It is logical to assume that even without activation, in a dormant state, a spore also possesses the ability to accumulate and/or release ions in response to environmental changes. This ability is referred to as the concept of natural ionic reservoir. Spores of all *Bacillus* species seem to be complex, multilayered ionic reservoirs:

(i) The spore core housing the DNA complexed with small acid-soluble proteins[26] is surrounded by a membrane which may have a limiting permeability[27] not only for large molecules, but also for ions.

(ii) The spore cortex is a thick but loosely cross-linked layer.[28,29] It is thought that the spore cortex is the major structural element of controlling the water content inside the core.

(iii) The spore coat is a multilayered protein shell encasing the cortex and protecting the spore from mechanical damage and harmful chemicals.

(iv) In addition, most species may possess an exosporium for which its function is so far unclear.

A hydrogel-like structure and its ionic sensitivity may be attributed to all integuments of the spore. The analogy of the spore cortex with ionic hydrogel is straightforward. The spore

* Corresponding author. Phone: (914) 773-3774. Fax: (914) 773-3418. E-mail: skazakov@pace.edu.
† Pace University.
‡ Burke Medical Research Institute.

10.1021/jp077188u CCC: $40.75
Published on Web 02/05/2008

cortex is a peptidoglycan polymer located between the spore inner and outer membranes. The cortex possesses a negative net charge. The low degree of cross-linking[30,31] supposes that the spore cortex is able to change volume in response to ionic changes as a result of balancing the electrostatic interactions of charged peptidoglycan chains and their network elasticity. It has been proposed earlier[32] that biopolymers in the spore core are cross-linked to form an ion-sensitive gel-like structure. The spore coats also have the protein-borne structures resembling biopolymer networks.[33]

By analogy with synthetic ion exchangers (hydrogels), the total number and type of ionizable groups inside a spore defines its ionic capacity. In the beginning of this study, there was no quantitative information available on the amount and type of ionizable groups for any species of dormant spores. Nevertheless, the presence of a significant amount of ionizable groups inside the spore has been obvious to predict that all constituents of spores contain charged groups fixed on the macromolecular chains. For example, a high density of negative charges inside the spore core can be associated with large amounts of dipicolinic acid (DPA, a spore specific component) and free glutamic acid (5−15% of dry weight of the spore core is DPA[33−37]). A negative charge of the spore cortex can be associated with the alternating glycan chains of β−1,4 linked *N*-acetyl-glucosamine and *N*-acetylmuramic acid residues generally forming the peptidoglycan matrix. (About 47% of the muramic acid residues is present in the cortex as a spore-specific muramic D-lactam, 18% is substituted with L-alanine residues, and 35% is with a peptide chain.[29] D-lactam residues are distributed predominantly near the alternate disaccharide residues.[38] 31−37% of these chains are involved in cross-linking.[30]) Even on the basis of those data, it looks obvious to suggest that carboxyl groups are present inside the spore matrix. Indeed, we found in literature[39] one suggestion that the ionizable groups present inside a spore are mostly carboxyl groups; however, to the best of our knowledge, there are no direct quantitative evidence on this fact in the literature.

This work aims to find these quantitative characteristics experimentally and predict the distribution of free counter-ions (protons) and co-ions (chloride ions) between interior and exterior of the dormant *Bacillus subtilis* spores, a model natural ionic reservoir. Experimentally, we measured the equilibrium pH in the exterior to *Bacillus subtilis* spores for different concentrations of spores and different concentrations of protons. Theoretically, the concentrations of bound and mobile protons inside the spore were found as functions of the concentration of protons added. The distribution of co-ions (chloride ions, the mobile ions of the same sign as that of the fixed charge on the spore matrix) between spores' interior and exterior was predicted from the Donnan equilibrium.

Our interest was also in the transitional kinetics of approaching the ionic equilibrium in the spores' suspension, since the mobility of ions within distinct spore structural compartments may be different.[40] For example, dielectric properties of *B. cereus* and *B. megaterium* spores[41,42] indicated that small ions within the spore protoplasts (core) exhibit the extremely low mobility ("electrostasis") whereas the spore cortex appears to contain a high concentration of mobile ions. Mostly, this difference was associated with probably complete permeability of spores to water.[40] However, the access of other molecules to the spore interior may be restricted by their size, hydrophobicity, and binding affinity.

By using the pertinent method developed[43] for studying the ion transport through the surface of micro- and nanosized hydrogel particles, time-resolved measurements of pH external to the *Bacillus* spores were performed. The kinetics of proton exchange between spores and surrounding aqueous solution has never been studied. One can suppose that the kinetics may be much more complicated than that in hydrogel suspensions mostly because of two coupled factors: a presumably high negative net charge and a multilayered structure of the spore matrix. In this work, we analyzed the proton exchange kinetics and found that the characteristic times were lasting from fractions of a second to thousands of seconds (hours). Herein, the longest diffusion times were assigned to the fluxes of protons in and out the spore core. In agreement with the recent observations[27] of the inner membrane lipids immobility in dormant bacterial spores, our results on the effective diffusion coefficients in the spore core and cortex indicate that the spore inner membrane between the spore cortex and core might be a major permeability barrier for protons to pass into the core.

Experimental Section

Sporulating Cultures and Spore Treatments. The *Bacillus subtilis* strain (1A700) used in this study was available from the culture collection of the Department of Microbiology at the University of Alabama (Birmingham, AL). *Bacillus subtilis* 1A700 possesses high sporulation efficiency. The strain was inoculated into the Difco sporulation medium (DSM), and the bacteria were grown to the beginning of sporulation (t_0). After exposing for an additional 48 h at 37 °C, the culture was harvested by centrifugation (Beckman Avanti J25) for 10 min at 10 000 × g and 4 °C. For spore purification, we used the method of lysozyme treatment and salt-detergent washes as described in ref 44. The pellet was treated with 1 M KCl/0.5 M NaCl solution. Lysozyme treatment was done by suspending the spores for 1 h at 37 °C in Tris-HCl buffer (50 mM, pH 7.2), containing 50 μg/mL lysozyme. The spores were cleaned by alternate centrifugation (10 000 × g, 10 min) of their suspensions in 1 M NaCl, deionized water, SDS (0.05%) solution, and TEP buffer (50 mM Tris-HCl buffer, containing 10 mM EDTA and 2 mM phenylmethylsulfonyl fluoride, pH 7.2), respectively. Finally, the spores were washed at least three times with deionized water. The spores were stored in deionized water at 4 °C. The stock suspension of *B. subtilis* spores had the pH ∼ 8.8. Sodium phosphate monobasic and dibasic, Trizma base, Trizma hydrochloride, lysozyme for spore purification, and nonionic detergent Tween 20 were from Sigma (St. Louis, MO). The sporulation medium (DSM) was obtained from DIFCO Laboratories (Detroit, MI). Chemicals were used directly without additional purification. Water purified by Milli-Q (Millipore) with pH 5.5−6.1 was used in all experiments.

Concentration of Spores. The concentration of spores was determined spectroscopically by measuring absorbance at 600 nm using a Lambda 2 UV−vis spectrometer (Perkin-Elmer, GmbH.) and microscopically using a digital optical microscope DC3−163-PH (Microscope World, CA). The stock suspension of *B. subtilis* spores was gradually diluted up to 20 times. The measured absorbance was plotted against factor (ϵln), where ϵ is the known extinction coefficient for the spores $\{2 \times 10^{-12}$ L/(spores·cm)[44]$\}$, l is the length of the cuvette ($l = 1$ cm), and n is the factor of dilution. The slope of the linear line gives the concentration of the stock suspension. The initial concentration of the stock suspension of *B. subtilis* spores was determined spectroscopically to be of $C_{sp}^0 = 1.18 \times 10^{12}$ sp/L. Microscopic determination of the spore concentration included the deposition of the 0.5−1 μL controllably diluted stock suspension between the glass and cover slides and the calculation of the number of

spores under the microscope. The microscopically determined concentrations of spores in the stock suspension were varied within a 2% interval around the one determined spectroscopically. All concentration measurements were carried out at room temperature (~25 °C).

pH Measurements. The setup for pH measurements provided the injection of acid, base, or spore suspension into the inner volume without perturbations of a MI-710 microcombination electrode (Microelectrodes Inc., Bedford, NH). The electrode was stored over nights in an acid buffer of pH 4. The electrode was calibrated in three IUPAC standard buffers at pH 4, 7, and 10 prior to each use. A Vernier Logger Pro software (version 2.3) was used for data acquisition, analysis, and storage.

The potentiometric titration of pure water and aqueous suspension of spores was performed with 0.1 M HCl. In this work, we did not perform the back-titration with NaOH to avoid an addition of sodium ions. The aqueous suspension of spores was taken as a starting point of the titration. Milli-Q water with initial pH ~ 5.85 was used for the reference titration. A sample was stirred by a stirring bar (1.5 × 2 × 5 mm) at ~70 rpm during titration. The initial volume of pure water or spores' suspension was 1.0 mL placed in the well. The equilibrium pH was recorded in 2 h after spores or acid injection. All measurements were carried out at room temperature (~25 °C). The theoretical curve for acid titration of pure water was calculated as follows: $\mathrm{pH} = -\log(10^{-5.85} + [\mathrm{HCl}])$, where $[\mathrm{HCl}] = (0.1\ \mathrm{M} \times \upsilon_{add})/(V_0 + \upsilon_{add})$, V_0 is the initial volume of water, υ_{add} is the volume of 0.1 M HCl added. The initial concentration of protons was calculated as follows: $[H^+]_{add} = (0.1\ \mathrm{M} \times \upsilon_{add} + 10^{-\mathrm{pH}_{sp}} \times V_{sp})/(V_{sp} + \upsilon_{add})$ in the case of acid injection into a spore suspension and $[H^+]_{add} = (10^{-5.85} \times V_0 + 10^{-\mathrm{pH}_{sp}} \times V_{sp})/(V_{sp} + V_0)$ in the case of spore injection into pure water, where V_{sp} and pH_{sp} are the volume and pH of a spore suspension injected. Final concentration of spores was adjusted after each injection: $C_{sp} = C^0_{sp} \times V_{sp}/(V_{sp} + V_0)$.

The response time of the pH electrode was tested by measuring pH changes in distilled water after acid or spores injections. A 1 mL sample of water or spore suspension was poured into the cuvette. The pH was equilibrated upon stirring. After 30−100 s of recording the signals, acid or spore suspension was injected into the cuvette. The measurements were carried out with a sample time of 0.1 s. It was found that the final pH equilibrates in ~10 s after acid injection. This interval includes both response time of the microelectrode and equilibration time of $[H^+]$ concentration (stirring and diffusion) in the volume tested. The minor leakage of $[H^+]$ through the glass surface of microelectrode is also possible.

When a certain amount of spores is injected into the aqueous solution, the accumulation of protons by spores begins immediately after their injection, so that the relative changes in pH are limited only by the rate of electronic circuitry which seems to be significantly less than the sample time used (0.1 s). The methods used to analyze the pH−kinetic curves are discussed in Results.

Average Size of Spores. The average hydrodynamic radius of *Bacillus subtilis* spores in water suspension were measured using a dynamic light scattering (DLS) technique at room temperature (25 °C). The theory of DLS has been extensively reviewed elsewhere.[45,46] The DLS gives information about the diffusion coefficient of the moving particles. The so-called average hydrodynamic radius, $\langle R_h \rangle$, of the particles can be extracted from the DLS data using the well-known Stokes−Einstein relationship, which is a definition for an effective hydrodynamic sphere,

$$\langle R_h \rangle = k_b T/6\pi\eta D \quad (1)$$

where D is the diffusion coefficient, η is the viscosity of the solvent, T is the absolute temperature, and k_b is the Boltzmann constant. $\langle R_h \rangle$ characterizes hydrodynamic interactions between particles and solvent and indicates how deeply a particle is drained by the solvent: a deep draining causes a reduction in $\langle R_h \rangle$; on the other hand, if only shallow draining is possible, $\langle R_h \rangle$ can become larger and larger.

Photon correlation spectroscopy (PCS) is the most common way to analyze the size distribution of submicron particles. In this work, light scattering measurements of the spore size were carried out on a "PhotoCor Complex" photon correlation spectrometer (PhotoCor Instruments Inc., MD) utilizing a 10 mW He−Ne laser (model 1135P, Uniphase Corporation, USA) as a light source. The thermostat and the cell holder are coaxial with z axis of the precise goniometer. The photodetecting system comprises the efficient receiving optics, low-noise photomultiplier tube operating in a photon counting regime, and amplifier−discriminator (AD). The output signal of the photodetecting system is analyzed by the single-board digital correlator with programmable number of channels in linear (128) and multi-tau (256) regimes. The measurements were done at the constant scattering angle of 90°.

Suspensions of spores were diluted to the concentration of 2.3×10^{10} sp/L and filtered into a cylindrical glass cuvette (Ø10 mm) using a 2 μm Millipore Millex filter. Thus prepared spore suspensions seemed to be convenient objects for DLS study since they had a uniform size distribution and their field−field correlation function was close to single-exponential. The quality of measurements was checked over the apparent signal-to-noise ratio of the autocorrelation function, overflow count, and baseline error. The cumulant analysis was successfully used to give the average size and polydispersity of spores. In addition, particle size distribution analysis with an automatic or visually assisted choice of a regularization level was carried out using the DynaLS software (ver. 2, Alango Ltd., Israel). Measurements of the hydrodynamic radius and integral scattering intensity were performed every 1 min (signal accumulation time, −50 s; interval between measurements, −10 s) over a course of 30 min. The reported spore size is the result of averaging those 25−30 measurements.

Experimental Results

Spores Characterization. The average hydrodynamic radius of the *B. subtilis* spores in the suspension containing 2.3×10^{10} sp/L was measured to be of (629 ± 5) nm at pH 7.5. This value was in good qualitative agreement with optical microscopic observations.

Bulk Titration of Spores' Aqueous Suspensions. There are two ways to expose spores to hydrogen ions, namely, injecting spores into the water with different pH values (dilution) or injecting different amount of acid into the spore suspension (titration). Prior to this study, it was unclear if those methods give equivalent results. Since any additional counter-ions or co-ions could drastically increase the complexity of the physicochemical pattern of proton exchange within the spore interior, we did not use NaOH for titration and limited our experiments to HCl titration.

In the first experiment (dilution), a known amount of the spores was successively injected into a vial with water of pH 5.85 ($[H^+] = 10^{-5.85}$ M). The pH was measured after at least 2 h of equilibration. As Figure 1 shows, a small amount of injected spores drastically increases the pH of the mixture. The spores

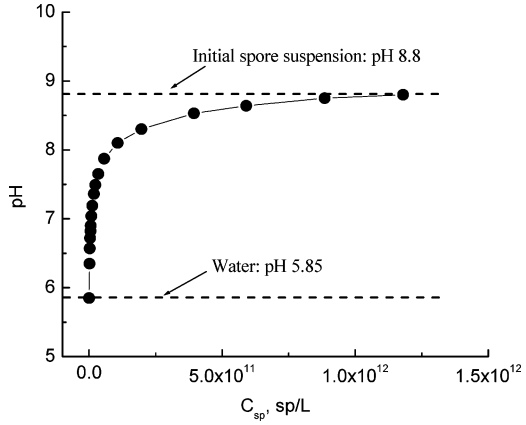

Figure 1. Variation of pH with concentration of *B. subtilis* spores injected into distilled water.

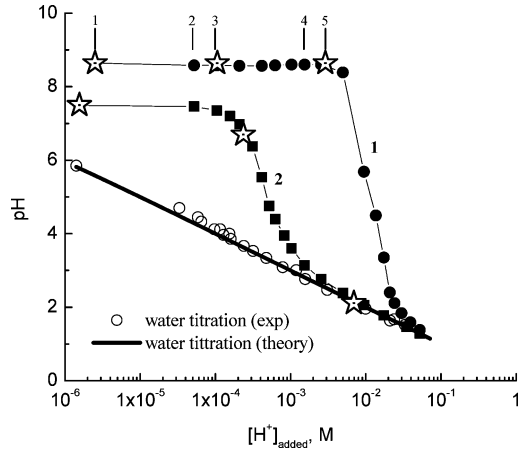

Figure 2. Changes in pH during the acid titration of pure water (○) and two suspensions of different concentration of *B. subtilis* spores: 1−5.9 × 10^{11} sp/L, 2−2.3 × 10^{10} sp/L. The stars and numbered vertical bars indicate the samples selected for kinetic measurements (see text and Figures 4 and 6).

consume the large portion of H^+ so that the pH of the mixture almost reaches the level of that for the initial spores' suspension. The results of this experiment are an unequivocal indication that spores are able to accumulate hydrogen ions and act as ionic reservoirs.

In the second experiment, acid titration of the suspensions of two different concentrations of spores was carried out as follows. A known amount of hydrogen ions was added to the suspension of a known amount of spores. If there were no consumption of H^+ by spores, then their titration curve would look like the titration curve of pure water (see Figure 2). If a significant amount of added hydrogen ions are consumed by the interior of spores, one can expect that the final concentration of H^+ will be less than that for pure water or, in other words, equilibrium pH will be higher than for pure water.

In Figure 2, the titration curves obtained for the spores' suspensions of two distinct concentrations are compared with the titration curve for pure water. The comparison clearly indicates that the significant amount of hydrogen ions is consumed by spores; that is, there should be a significant number of charged sites (ionizable groups) fixed within each spore to bind this amount of H^+. In Discussion, we will estimate the number of binding sites for H^+ in the spore interior.

Time-Resolved pH Measurements. By analogy with ionic hydrogels,[43] two possible processes can affect the proton concentration in the solution external to a spore: (i) the fast binding of the ions to immediate surface of each spore and (ii) the successive shift of the diffusion front of bound ions into the deeper interior layers of a spore. Both processes are associated with the binding of ions to the ionizable groups and redistribution of the mobile ions between the spore interior and the spore exterior. Obviously, the overall kinetics should contain the features of ion exchange between the spore structural sublayers.

In order to understand if a pH microelectrode is capable of resolving a time-course of pH changes in the external solution in the presence of spores, acid injections were performed to the spore suspension. In Figure 3a, the proton consumption by spores is compared with the time course of pH changes in pure water after the addition of acid into both samples under the same experimental conditions. As one can see, pH sharply drops toward the level of pure water, but when hydrogen ions start to bind to the ionizable groups on the surface of spores, pH begins to rise, finally almost reaching the initial pH level.

To visualize the difference between the time courses of external pH in pure water and that in the spore suspension, time was presented in a logarithmic scale, whereas pH was recalculated into the proton concentration also presented in a log scale (Figure 3b). The discrepancies between the two curves begin at the first second indicating a higher rate of proton consumption by spores in comparison with the rate of the external pH equilibration proceeding simultaneously during the first 10 s after the acid addition. This perturbation of proton kinetics by the pH equilibration ("instrumental" effect) does not allow one to analyze the initial part of the curve numerically. Nevertheless, the nonlinear shape of curve (2) for time >10 s in a log−log scale (Figure 3b) shows that even the slow process is not single-exponential. The part of the curve for time >30 s was extracted and fitted into a two-exponential function (2) to estimate the time constants for those two significantly slower processes:

$$[H^+] = [H^+]_0 + A_1 \exp(-t/\tau_1) + A_2 \exp(-t/\tau_2) \quad (2)$$

where $[H^+]_0$ is the equilibrium external concentration of protons, τ_1 and τ_2 are the corresponding time constants. The results of fitting are as follows: (i) the regression factor is $R = 0.999$, (ii) the obtained value of $[H^+]_0$ corresponds to $pH_0 = 8.71$ which is in good agreement with the experimental pH = 8.8 ± 0.1, (iii) two time constants are equal to (239 ± 1) s and (783 ± 5) s, respectively, and (iv) the fitting curve is shown in Figure 3b as a dashed line (3).

The data obtained within the first 10 s may probably point out two more processes. A few injections of different concentrations of protons to the same amount of spores were undertaken to clarify this point at least qualitatively. All samples present in Figure 4 correspond to a plateau of the titration curve shown in Figure 2. A comparison of the $[H^+]_{out}$−kinetic curves leads to a conclusion that the acid addition changes the external $[H^+]_{out}$ in opposite direction as the consumption of protons as spores do at the very early moment; that is, protons spread around tending to increase $[H^+]_{out}$, whereas their binding to the surface of spores decreases $[H^+]_{out}$. Both processes can compensate for each other as it can be seen (curve 1), when a small amount of protons is added. On the other hand, when a significant amount of protons has been added (curve 5), the rate of their binding to the spore surface can be much higher than the rate of their slow penetration and binding within the spore, so that the concentration of mobile protons inside spore but close to its surface may be much higher than it can be held thermodynamically. To compensate this strong nonequilibrium gradient, the efflux of mobile protons appears on the first second after acid

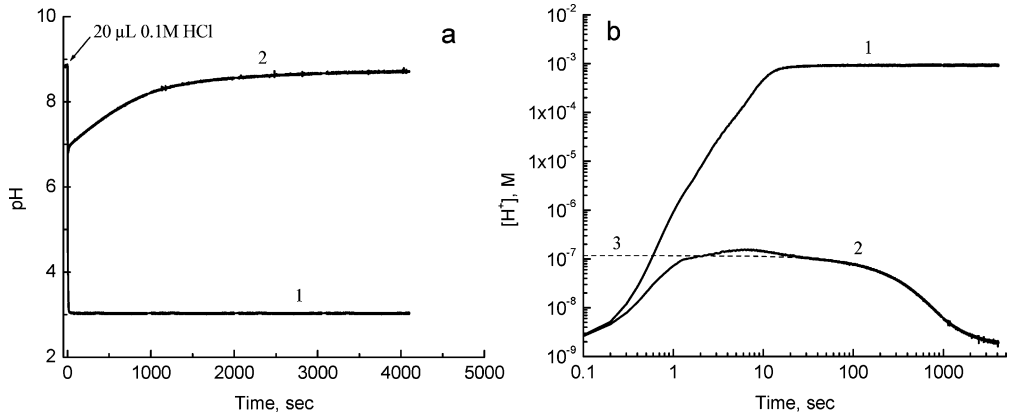

Figure 3. Time courses of external pH (a) and proton concentration (b) measured after addition of 20 μL of 0.1 M HCl into (1) 1 mL of pure water and (2) 1 mL of the *B. subtilis* spore suspension with concentration 5.9×10^{11} sp/L. The arrow indicates the moment of acid injection. The dashed curve (3) is the fitting curve calculated by two-exponential function. The solid curves (1) and (2) are the experimental data.

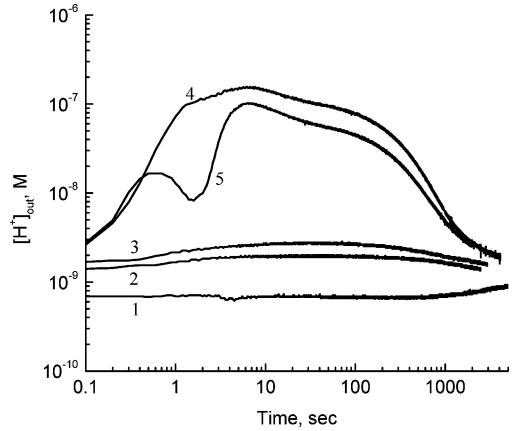

Figure 4. Time courses of external proton concentrations measured in the *B. subtilis* spore suspensions prepared as follows: (1) 0.5 mL of water was added to 0.5 mL of spore suspension, (2) 5 μL of 0.01 M HCl was added to 1 mL of spore suspension, (3) 10 μL of 0.01 M HCl was added to 1 mL of spore suspension, (4) 20 μL of 0.1 M HCl was added to 1 mL of spore suspension, and (5) 25 μL of 0.1 M HCl was added to 1 mL of spore suspension. The same total concentration of spores 5.9×10^{11} sp/L was in all samples. These samples were indicated on the titration curve 1 (Figure 2) by numbered vertical bars.

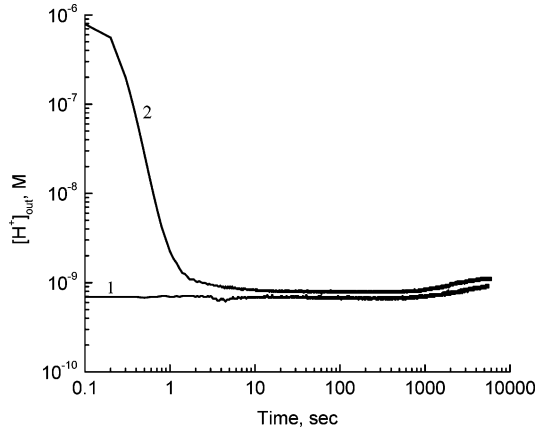

Figure 5. Time courses of external proton concentrations measured in the *B. subtilis* spore suspensions prepared as follows: (1) 0.5 mL of water was added to 0.5 mL of spore suspension, (2) 0.5 mL of spore suspension was added to pure water. The final concentration of spores was 5.9×10^{11} sp/L in both samples.

injection causing a minimum of $[H^+]_{out}$ in curve 5 (Figure 4). The characteristics of those fast processes cannot be extracted from these data numerically because they are accompanied by the diffusion of added protons.

To avoid the latter process, we considered the addition of spores to the acid solution with a known uniform concentration of protons. In this case, the consumption of protons by spores begins everywhere simultaneously, so that the early fast processes of proton binding to the spore surface can be easily revealed as demonstrated by Figure 5. The difference between two kinetic curves for similar but differently prepared samples is obvious. The addition of water to spore suspension changes the external pH in an opposite direction as the consumption of protons by spores does. On the contrary, in the course of spore addition to water, the consumption of protons by spores is the only process governing the pH external to spores. Bearing this finding in mind, the further pH−kinetic experiments in the spore suspensions were carried out by pouring spores into water with different pH adjusted by HCl.

pH Kinetics of *Bacillus subtilus* Spores. Figures 6 shows plots of the $[H^+]_{out}$ kinetics for spore suspensions of two different concentrations immerged into aqueous solutions of different pH. The samples are marked by stars on the titration

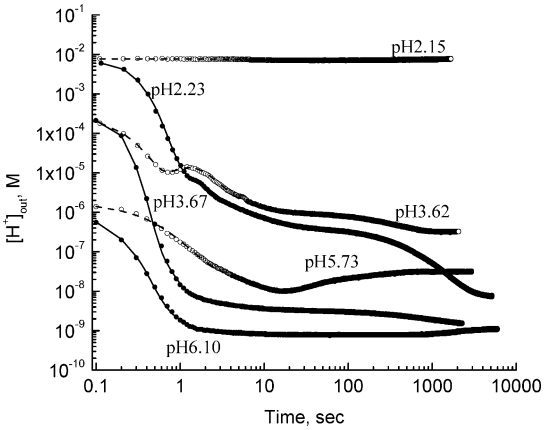

Figure 6. Time courses of external proton concentrations measured in the *B. subtilis* spore suspensions: (solid points and solid curves) prepared by injection of 0.5 mL of the stock suspension (1.18×10^{12} sp/L) into 0.5 mL of aqueous HCl solutions with the pH indicated for each curve and (open circles and dashed curves) prepared by injection of 20 μL of the stock suspension (1.18×10^{12} sp/L) into 980 μL of aqueous HCl solutions with the pH indicated for each curve. Points are the experimental data; curves are the fitting curves with the adjustable parameters listed in Table 1 (see Discussion for details).

curves in Figure 2. It can be seen that for all samples studied, the process of pH equilibration is a multistep one and requires more than 1 h to get the final value of pH external to spores. The following features of $[H^+]_{out}$−kinetic curves are observed:

(i) A fast decrease in $[H^+]_{out}$ during the first second after spores injection can be assigned to an intensive penetration of hydrogen ions most likely into the presurface layer of the spores. This might indicate that the surface of spores is negatively charged and may contain a significant amount of ionizable groups.

(ii) For the samples with a relatively high initial $[H^+]_{out}$, ($pH_{ini} \sim 2-3.6$, depending on the number of spores), the kinks with positive derivatives are observed on the $[H^+]_{out}-$kinetic curves around 1 or 2 seconds after spore injections. The positive derivative of the $[H^+]_{out}-$kinetic curve means that an efflux of protons appears. One can speculate that the processes of further penetration of hydrogen ions into the deeper structural layers of spores and their binding to ionizable groups are much slower than on the spore surface, so that too many protons are accumulated in the spore outer layer to be thermodynamically stable.

(iii) Definitely, there are several interplaying processes which slow down the kinetics of proton consumption by spores in the interval from singles to thousands of seconds. The balancing of these steps may decrease, increase, or even stop proton consumption depending on the concentration of protons and concentration of spores. Our assumption is that the kinetics of proton uptake is the result of coupling diffusion and binding processes. If so, more precisely, the shape of $[H^+]_{out}-$kinetic curve will depend not only on the proton concentration gradient but also on [n], the total concentration of ionizable groups inside a spore, that is, the total fixed charge of spore matrix.

Discussion

Equilibrium Binding of Protons to Ionizable Groups within Spores. The experimental results on dilution and bulk titration of spore suspensions may be utilized to determine the apparent binding constant K_{app} and the average number of binding sites (or ionizable groups) N for H^+ in the interior of each spore. To derive K_{app} and N from these data, it was assumed that the spores have negatively charged ionizable groups fixed on the spore matrix and are unable to move out of the spore. The ions of opposite sign, the counter-ions, are free to move through the boundaries between the spore structural layers (semipermiable membranes) and bind to fixed charged sites within the spore matrix. In principle, each structural layer of a spore may have a different concentration of fixed charges, but in our titration experiments, we measured a resultant effect of all internal layers on the final equilibrium distribution of protons between interior and exterior to the spore.

A similar model has been considered for the ionic hydrogels to calculate the concentration of all ions (bound and unbound, inside and outside) as a function of added acid or/and salt concentration.[1−11] Importantly, according to the Donnan theory, the concentration of fixed charged sites on one side of a semipermeable membrane affects the equilibrium distribution of all the mobile ions between two volumes separated by the membrane. For example, the concentration of counter-ions may be significantly higher inside the spore than that outside until all fixed charges are neutralized. In contrast, the concentration of co-ions, the mobile ions of the same sign as that of fixed charges of the matrix (in our case, chloride ions), may be much lower inside the spore than outside because of the Donnan exclusion effect.[47] The appropriate equilibrium distribution of counter-ions and co-ions for the spore related model can be given by the Donnan ratio

$$\lambda_D = \frac{[H^+]_{in}}{[H^+]_{out}} = \frac{[Cl^-]_{out}}{[Cl^-]_{in}} \quad (3)$$

where $[H^+]_{in}$, $[H^+]_{out}$, $[Cl^-]_{in}$, and $[Cl^-]_{out}$ are the concentrations of mobile counter-ions and co-ions, inside and outside the spore. Frequently, the difference in concentrations of free ions on both sides of the semipermeable membrane generates a swelling pressure within an elastic ion exchanger, but in this paper, we do not consider swelling/deswelling of the spore matrix.

The average number of binding sites for H^+ per each spore (N) is named as the spore's proton capacity. The total concentration of binding sites in spore suspension is related to the spore concentration as follows: $[Sn] = NC_{sp}/N_A$, where N_A is the Avogadro number. The concentration of binding sites per each spore is $[n] = [Sn] \times V/V_{sp}$, where V and V_{sp} are referred to the total volume of the suspension and the volume of all spores, respectively.

After injection of a known amount of spores (C_{sp}) into water with the known pH, or after addition of a known amount of protons ($[H^+]_{add}$) into a spore suspension with the known concentration of spores (C_{sp}), a portion of free protons from the external solution diffuse inside the spore and binds to the ionizable groups denoted as R:

$$H^+ + R^- \leftrightarrow HR \quad (4)$$

In equilibrium, the concentrations of unbound (dissociated) ionizable groups $[R^-]$, ionizable groups bound with hydrogen [HR], and free protons $[H^+]_{in}$ inside the spore are related by an equilibrium binding constant:

$$K = \frac{[HR]}{[H^+]_{in}[R^-]} = \frac{[HR]}{[H^+]_{in}\left([Sn] \times \frac{V}{V_{sp}} - [HR]\right)} = \frac{[H^+]_{bound}}{[H^+]_{in}\left([Sn] \times \frac{V}{V_{sp}} - [H^+]_{bound}\right)} \quad (5)$$

We have taken into account that the concentration of bound ionizable groups is equal to the concentration of bound protons, $[HR] = [H^+]_{bound}$, and the contribution of activity coefficients is ignored. Equation 5 yields the concentration of bound protons as a function of the concentration of free protons inside the spores:

$$[H^+]_{bound} = \frac{K[H^+]_{in}}{1 + K[H^+]_{in}}[Sn]\frac{V}{V_{sp}} \quad (6)$$

where [Sn] and K are the parameters of the well-known Langmuir isotherm. In the material balance equation in terms of the number of moles of added, free, and bound protons

$$[H^+]_{add} \times V = [H^+]_{out} \times (V - V_{sp}) + [H^+]_{in} \times V_{sp} + [H^+]_{bound} \times V_{sp} \quad (7)$$

we have used that the volume of water is $V_w = V - V_{sp}$. By combining eqs 6 and 7, the experimentally available difference between $[H^+]_{add}$ and $[H^+]_{out}$ is expressed as a function of the concentration of mobile protons inside the spore $[H^+]_{in}$:

$$\Delta[H^+] = [H^+]_{add} - [H^+]_{out} = ([H^+]_{in} - [H^+]_{out})\frac{V_{sp}}{V} + \frac{K[H^+]_{in}}{1 + K[H^+]_{in}}[Sn] \quad (8)$$

Equation 8 implies that, if $[H^+]_{in}$ is known for each titration point, all data in Figures 1 and 2 could be presented on the same scale in terms of $\Delta[H^+]$ versus $[H^+]_{in}$ and further fitting would give [Sn] and K as adjustable parameters. Since it was impossible to measure the concentration of mobile ions inside a spore, and $[H^+]_{in}$ can be unequal to $[H^+]_{out}$, we have considered two specific cases to find these parameters.

Spore's Proton Capacity. At high concentrations of added protons, when the major portion of biding sites is protonated and the concentration of fixed charges $[R^-]$ approaches zero, the concentrations of mobile protons inside and outside the spores are expected to be equal. This is a range where $K[H^+]_{in} \gg 1$, and the experimental points for spore suspensions coincide with the titration curve for pure water as shown in Figure 2. It follows from eq 8, that if $K[H^+]_{in} \gg 1$ and $[H^+]_{in} \approx [H^+]_{out}$,

$$\Delta[H^+] = [H^+]_{add} - [H^+]_{out} \approx [Sn] \quad (9)$$

that is, $\Delta[H^+]$ does not depend on $[H^+]_{out}$ and gives the value for the total concentration of binding sites in spore suspension $[Sn] = NC_{sp}/N_A$.

To find the average number of binding sites for H^+ per each spore (N), we have represented the number of hydrogen ions (bound and unbound) penetrated into a spore $N_A\Delta[H^+]/C_{sp}$ in Figure 7 as a function of $[H^+]_{out}$ for the two concentrations of spores. It was observed that $N_A\Delta[H^+]/C_{sp}$ can be regarded as constant, when $[H^+]_{out}$ exceeds 10 mM. The data above this value have been averaged to provide the spore proton capacity estimate as $N = (2.18 \pm 0.10) \times 10^{10}$ sites per spore (dashed line in Figure 7).

Taking into account that volume of each spore is about 10^{-15} L ($r \sim 629$ nm), one can estimate that the concentration of proton binding sites per spore [n] $\approx$ 35 M.

Equilibrium Binding Constant. Let us consider eq 8 when $K[H^+]_{in} \ll 1$. One can easily show that

$$\Delta[H^+] = [H^+]_{add} - [H^+]_{out} \approx ([H^+]_{in} - [H^+]_{out})\frac{V_{sp}}{V} + K[Sn][H^+]_{in} \quad (10)$$

that is, $\Delta[H^+]$ is linearly proportional to $[H^+]_{in}$. Our dilution data presented in Figure 1 may correspond to this case because the concentrations of added protons $[H^+]_{add}$, and therefore, mobile protons inside the spores $[H^+]_{in}$ may be low enough to make $K[H^+]_{in} \ll 1$. Moreover, in the course of spore dilution by pure water, the only mobile ions in the system are H^+ and OH^-, and eq 10 is simply the balance equation for a solution of a weak acid at concentration [Sn] and binding constant K, so that one can assume that $[H^+]_{in} \approx [H^+]_{out}$.

These assumptions were proved by plotting $\Delta[H^+]/[Sn]$ as a function of $[H^+]_{out}$ for the dilution data (Figure 8). Note that the total concentration of binding sites in spore suspension $[Sn] = NC_{sp}/N_A$ has been found in the previous section. As one can observe, the experimental points are satisfactorily fitted into the linear function (confirming $K[H^+]_{in} \ll 1$) passing through the origin (confirming $[H^+]_{in} \approx [H^+]_{out}$). In accord with eq 11,

$$\Delta[H^+]/[Sn] \approx K[H^+]_{out} \quad (11)$$

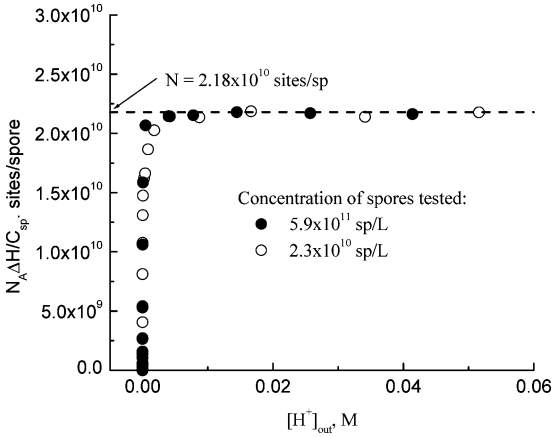

Figure 7. Plot of the number of hydrogen ions (bound and unbound) penetrated into one spore $N_A\Delta[H^+]/C_{sp}$ as a function of the outer concentration of free protons, $[H^+]_{out}$, for two different amount of spores in 1 mL suspension. The dashed line indicates the level of the average number of binding sites within each spore.

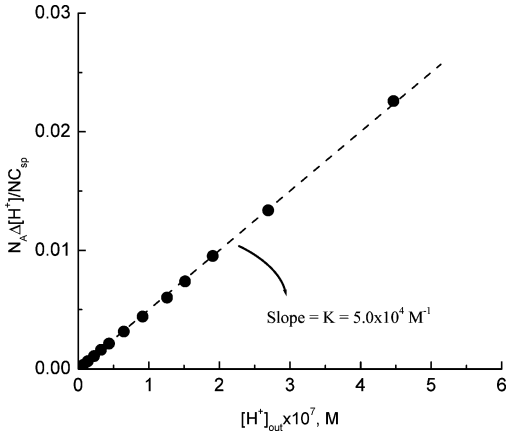

Figure 8. Plot of the difference between the concentrations of added protons $[H^+]_{add}$ and free protons $[H^+]_{out}$ in the external solution normalized by the total concentration of spores [Sn] as a function of $[H^+]_{out}$. The dashed line is the fitting curve $Y = KX$ with K indicated.

the slope of the line gives us the value of the apparent binding constant $K_{app} = (5.0 \pm 0.2) \times 10^4$ M^{-1}. The value corresponds to the apparent dissociation constant $K_a = (2.0 \pm 0.1) \times 10^{-5}$ M or the apparent $pK_a = 4.7 \pm 0.2$, where the apparent pK_a of the spore matrix is defined as the internal $pH_{in} = -\log([H^+]_{in}$, at which 50% of ionizable groups inside the spore are dissociated. Remarkably, the obtained value of apparent pK_a for the *B. subtilis* spore is comparable to those of individual monomers and cross-linked polymer matrix with carboxyl groups: the pK_a of acetic acid is 4.75,[48] that of acrylic acid is 4.75,[49] that of methacrylic acid is 4.66,[50] and that of poly(methacrylic acid) hydrogel microspheres is 4.7[4] in water at 25 °C. This comparison allows us to ascribe the negatively charged groups fixed in a spore matrix to carboxyl groups.

Model Predictions of the $[H^+]_{in}$. Because the ratio V_{sp}/V is not greater than 10^{-3} for all concentrations of spores studied in this work, the first term in eq 8 is small and can be neglected in comparison with the second one. Thus, for the known [Sn] and K, rearrangements of eq 8 result in the following equation for $[H^+]_{in}$,

$$[H^+]_{in} \approx \frac{\Delta[H^+]}{K([Sn] - \Delta[H^+])} \quad (12)$$

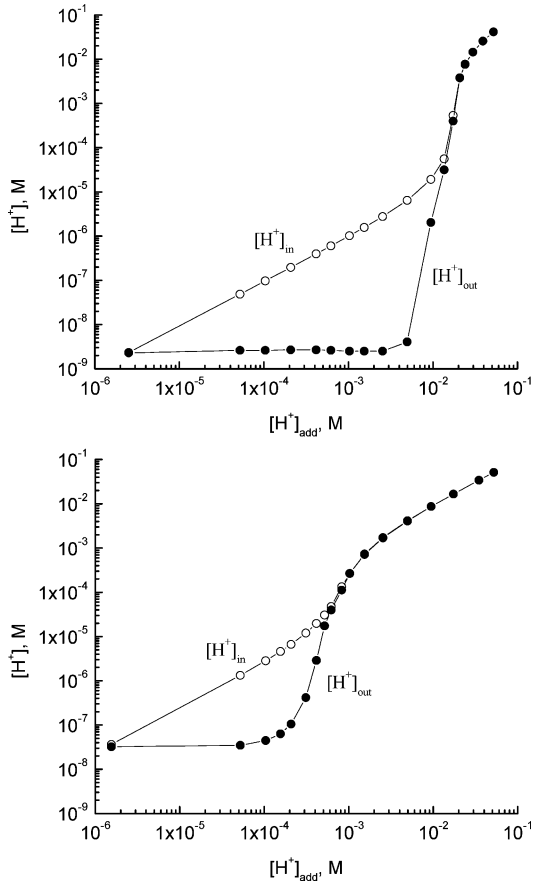

Figure 9. Comparison of the predicted concentrations of unbound protons inside the spores $[H^+]_{in}$ with the measured concentrations of free protons outside the spores $[H^+]_{out}$ as functions of added concentration of protons $[H^+]_{add}$ to the aqueous suspensions with the following concentrations spores (a) 5.9×10^{11} sp/L and (b) 2.3×10^{10} sp/L.

The results of $[H^+]_{in}$ calculations are compared with $[H^+]_{out}$ in Figure 9 a,b for two different initial concentrations of *B. subtilis* spores.

In 1980, Setlow and Setlow found for *B. cereus* and *B. megaterium*[24,25] species that the pH value within dormant spores was in the range of 6.3−6.5 when the external pH changed in the range of 8.4−7.1. We studied a range of the external pH varying from 1.3 to 9 for *B. subtilis* spores to show that, in general, the internal pH is dependent on the concentration of protons added, the concentration of spores in the suspension, and hence, the degree of protonation of the ionizable groups. Herein, the concentration of free hydrogen ions inside the spore can be up to 3 orders of magnitude higher than that outside the spore.

The difference between $[H^+]_{out}$ and $[H^+]_{in}$ decreases when the concentration of added protons $[H^+]_{add}$ becomes high; that is, $[H^+]_{in}$ becomes equal to $[H^+]_{out}$ when all ionizable groups are protonated. On the other hand, one can always consider that the internal and external pHs are the same if the spores are diluted by pure water, that is, no co-ions are added.

In accord with the Donnan exclusion effect and eq 3, the chloride ion concentrations are reversal to the proton concentrations on both sides of a spore surface, so that in the external solution, $[Cl^-]_{out}$ may be 3 orders of magnitude higher (depending on the spore concentration) than that within the spore (Figure 10). It is worthy to note that an electrochemical potential gradient between the interior and the exterior of spores may exist to oppose chloride co-ions entry into the spore until all ionizable groups within the spore matrix are neutralized.

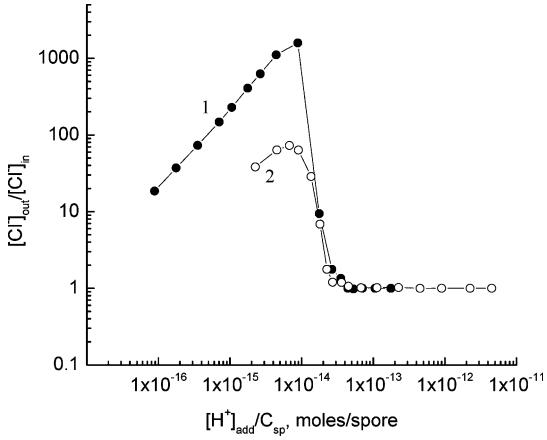

Figure 10. Predicted ratio of the chloride ion concentration outside to that inside the *B. subtilis* spores as a function of added amount of protons per each spore: (1) 5.9×10^{11} sp/L and (2) 2.3×10^{10} sp/L.

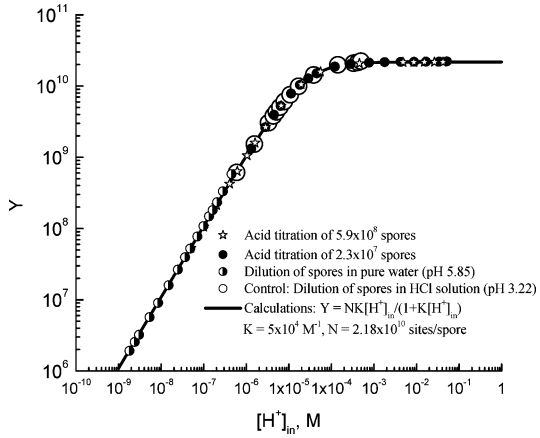

Figure 11. Model predicted number of protonated sites per *B. subtilis* spore versus the concentration of free hydrogen ions within a spore for all sets of titration and dilution data. The solid line has been calculated using eq 13.

Now, so long as we know $[H^+]_{in}$ for each titration point, all data points in Figures 1 and 2 have been plotted on the same scale in terms of $\Delta[H^+]$ versus $[H^+]_{in}$. to show that they belong to the same curve which was well-described by the Langmuir isotherm (eq 13) rearranged from eq 8, when $V_{sp}/V \ll 1$,

$$Y = ([H^+]_{add} - [H^+]_{out}) \times \frac{N_A}{C_{sp}} = N\frac{K[H^+]_{in}}{1 + K[H^+]_{in}} \quad (13)$$

A control experiment has been performed as follows: pH of 1 mL of water was adjusted by 0.1 M HCl in a few vials to have a final pH of 3.22; then, a different amount of spores was suspended in each vial, sonicated for 2 min, and left sealed in a cold room (4 °C) overnight; the equilibrium pH was measured after ∼10 h at room temperature. Figure 11 shows that all experimental points (for titration, dilution, and control experiments) fall down the same calculated curve, which is the Langmuir isotherm with numerical values of N and K derived in the previous sections of this paper. This result may be regarded as a validation of the approach to characterize dormant spores as ionic reservoirs with the equilibrium binding constant K and the average number of binding sites independent of the concentration of spores.

Kinetics of pH Equilibration in Spore Suspension. To describe pH equilibration shown in Figures 6 quantitatively, a kinetic model of relaxation to equilibrium was applied. The

TABLE 1: Fitting Parameters of the Kinetic Curves for External Proton Concentrations Measured in the *Bacillus subtilis* Spore Suspensions of Two Different Spore Amounts with Different Initial pHs

	$C_{sp} = 5.9 \times 10^{11}$ sp/L			$C_{sp} = 2.3 \times 10^{10}$ sp/L		
parameter	pH 6.10	pH 3.67	pH 2.23	pH 5.73	pH 3.62	pH 2.15
$[H^+]_{eq}$	1.1×10^{-9}	1.4×10^{-9}	7.5×10^{-9}	3.1×10^{-8}	3.2×10^{-7}	8.7×10^{-3}
A_1, M	2.0×10^{-6}	8.0×10^{-3}	4.7×10^{-2}	1.8×10^{-6}	6.8×10^{-3}	3.2×10^{-3}
τ_1, sec	**0.09**	**0.05**	**0.11**	**0.3**	**0.25**	**4.0**
A_2, M	-5.2×10^{-7}	-1.6×10^{-2}	-5.5×10^{-2}	-5.0×10^{-7}	-6.5×10^{-3}	-2.6×10^{-3}
τ_2, sec	**0.06**	**0.03**	**0.07**	**0.29**	**0.26**	**3.2**
A_3, M	1.1×10^{-8}	1.34×10^{-6}	2.3×10^{-5}	8.0×10^{-7}	6.0×10^{-5}	2.0×10^{-5}
τ_3, sec	**0.4**	**0.2**	**1.0**	**0.65**	**1.0**	**3089**
A_4, M	2.0×10^{-10}	5.0×10^{-9}	1.2×10^{-6}	-3.0×10^{-7}	2.1×10^{-6}	-3.2×10^{-7}
τ_4, sec	**8.0**	**3.0**	**8.0**	**0.59**	**5.6**	**3809**
A_5, M	1.5×10^{-10}	7.0×10^{-10}	2.49×10^{-7}	1.7×10^{-7}	6.9×10^{-7}	
τ_5, sec	**803**	**322**	**252**	**8.9**	**250**	
A_6, M	-5.2×10^{-10}	1.2×10^{-9}	1.64×10^{-7}	-1.4×10^{-7}		
τ_6, sec	**2007**	**1164**	**693**	**11**		
A_7, M				-1.8×10^{-8}		
τ_7, sec				**175**		

kinetics of proton binding inside hydrogels after acid addition has been described in ref 43 by three reversible reactions with three "types" of protons in the three-layered system: free protons in the external solution, protons bound to the hydrogel surface site, and protons bound in the bulk of hydrogel. Let us represent the kinetics of proton penetration into the multilayered interior of spores as a set of n monomolecular reversible reactions

$$X_0 \underset{k_{-1}}{\overset{k_1}{\rightleftharpoons}} X_1 \underset{k_{-2}}{\overset{k_2}{\rightleftharpoons}} .... \underset{k_{-n}}{\overset{k_n}{\rightleftharpoons}} X_n \qquad (14)$$

where n is not known a priori, X_0 is a free proton in the external solution, X_i is a proton bound in a distinct layer of the spore structure, and k_i and k_{-i} are the rate constants for the forward and reversible binding reactions, respectively. It is known from chemical kinetics[51] that the solution of the system of n linear differential equations of the first order for this scheme is the superposition of n exponential functions

$$X_i = X_i^{eq} + \sum_{j=1}^{n} A_{ji}\, e^{-t/\tau_j} \qquad (15)$$

where X_i^{eq} is the equilibrium concentration of protons, A_{ji} are the factors which contain the rate constants and depend on the initial conditions, τ_j are the characteristic times of the processes and are the functions of all rate constants k_i, k_{-i}. Values of τ_j can be found from the experimental data for any of concentration $[X_i]$ as a function of time. It is essential to note that the number of exponentially decaying functions corresponds to the number of reversible processes involved into equilibration.

In our experiment, the concentration of protons in exterior to spores, $[H^+]_{out}$, was measured as a function of time after spores' injection into the HCl solution with the known pH. The kinetic curves are present in Figure 6. The following important points are gleaned from the fitting parameters summarized in Table 1:

(1) The minimum number of exponential functions necessary to fit the data into eq 15 depends on the initial concentration of protons and the number of spores in the suspension, that is, on the initial gradient of the proton concentration between inside and outside of the spore and the total number of ionizable groups within the spore matrix. These experimental results suggest that the kinetics of hydrogen ions uptake into a spore is governed by two processes. One is proton diffusion driven by the concentration gradient. Another is proton binding to the charged spore matrix.

(2) The negative values of the pre-exponential factors mean that those terms in eq 15 describe the effluxes of protons. The coupling of influx and efflux of all ions involved into the ion exchange between spore and external solution sometimes appears on kinetic curves as the waving kinks, as one can see on the curves for pH 3.62 and pH 2.15. This is in contrast to pure diffusion, where the fluxes are not coupled, and the concentration gradients determine mass transport. Most likely all steps of proton kinetics revealed for spores result from a tiny balance between coupled in and out fluxes of ions. In some cases, however, the effect of the efflux may not be visible on the resultant kinetic curves and cannot be resolved by numerical procedure of fitting because the procedure of finding constituents from the integral experimental results generally is described as a so-called "ill-posed" problem.

(3) For a particular kinetic curve, the exponential functions with close values of the characteristic rates but with pre-exponential factors of different sign were attributed to the same step of the ion exchange kinetics. Four distinct time scales for proton uptake kinetics lasting from fractions of a second to thousands of seconds have been distinguished. If those kinetic steps are associated with the multilayered structure of spores, a relatively high difference between the characteristic times, reaching up to 4 orders of magnitude, supposes that the effective diffusion coefficients differ significantly in each layer.

The concept of the simultaneous diffusion and chemical reaction (for example, binding to ionizable groups) is not a new one. It was especially fruitful in describing the kinetics of ion diffusion concomitant with the volume change[52] as well as the kinetics of surfactant binding[53] in polymer gels. As it has been shown theoretically and experimentally, the diffusion processes are extremely complicated. The transitional kinetics of approaching the ionic equilibrium in the spores' suspension has never been studied, and Figure 6 provides evidence that ion exchange kinetics within the spore is much more complicated than the one in hydrogel microspheres.[43]

We follow the modeling of diffusion and binding in hydrogels in order to explain at least qualitatively the ion exchange kinetics in spore suspensions. To simplify the equations, it was assumed that (i) the process of ion binding to the polymer matrix is rapid in comparison to diffusion; that is, the local equilibrium always exists between free and bound ions; (ii) the diffusion coefficient of an ion in water D_{ion} is constant and does not vary with concentration and time; (iii) the changes in volume are negligible, and (iv) the concentration of protons at the diffusing front $[H^+]_{front}$ does not significantly change. Under these

TABLE 2: Values Used in Eq 15 and Calculated Effective Diffusion Coefficients for Protons in Spores

	numerical values						source of data
concentration of spores, sp/L	5.9×10^{11}	5.9×10^{11}	5.9×10^{11}	2.3×10^{10}	2.3×10^{10}	2.3×10^{10}	experiment
concentration of protons at the diffusion front, $[H^+]_{front}$, M	7.94×10^{-7} (pH 6.10)	2.14×10^{-4} (pH 3.67)	5.89×10^{-3} (pH 2.23)	1.86×10^{-6} (pH 5.73)	2.40×10^{-4} (pH 3.62)	7.08×10^{-3} (pH 2.15)	experiment
concentration of binding sites within a spore, [n], M	35	35	35	35	35	35	result of this paper
apparent binding constant, K, M^{-1}	5×10^4	5×10^4	5×10^4	5×10^4	5×10^4	5×10^4	result of this paper
diffusion coefficient for protons in water, D_{ion}, nm^2/s	9.38×10^9	9.38×10^9	9.38×10^9	9.38×10^9	9.38×10^9	9.38×10^9	taken from ref 4
effective diffusion coefficient, D_{eff}, nm^2/s	5.8×10^3	7.3×10^5	4.5×10^8	6.4×10^3	9.1×10^5	6.3×10^8	calculated using eq 17

assumptions, the effective diffusion coefficient in the case of binding is given by[52−54]

$$D_{\text{eff}} = \frac{D_{\text{ion}}}{1 + \dfrac{[n]K}{(1 + K[\text{H}^+]_{\text{front}})^2}} \tag{16}$$

where $[n]$ and K are the average concentration of binding sites in a spore and the apparent binding constant, respectively, as defined in the previous section. Equation 16 shows that the effect of proton binding to ionizable groups is in slowing the diffusion process. The degree to which the diffusion coefficients of protons are lowered inside a spore depends on the initial concentration of protons at the very beginning of proton uptake. The effective diffusion coefficient at the immediate vicinity to the spore surface was estimated for the spore suspensions studied. The values of the inputs to eq 16 are shown in Table 2. The results of calculations are present in the last row to show that the effect of binding on diffusion process may be substantially weakened when the concentration of protons at the diffusion front is high, and $K[\text{H}^+]_{\text{front}} \gg 1$.

The fast and slow time constants represented in Table 1 for different concentrations of spores and different initial concentrations of protons indicate the time for diffusion of protons through different layers of the spore, respectively. To calculate the effective diffusion coefficients in each spore structural layer, we estimated the thickness of outer coat, inner coat, cortex, and core for *B. subtilis* spore using its electron micrographs in Figure 1 of the review by Driks.[33] The contours of the spore compartments show (Figure 12) that a spore under an electron microscope is not spherical and the thickness of each layer varies along the spore surface. The areas edged by those contours have been calculated, and the average radius of each area has been estimated, as the radius of equivalent sphere. By using the art of the Motic 2000 image analysis software, the average thickness of outer coat is estimated to be 69 nm, that of inner coat is estimated to be 50 nm, that of the cortex is estimated to be 132 nm, and the average radius of the core is estimated to be 380 nm. The total average radius of the spore was estimated to be ~631 nm. We estimated the uncertainties to be not less than ±10 nm in those calculations, so that the value of the total average spore radius looks very close to the value observed in our DLS measurements (see the spore characterization section).

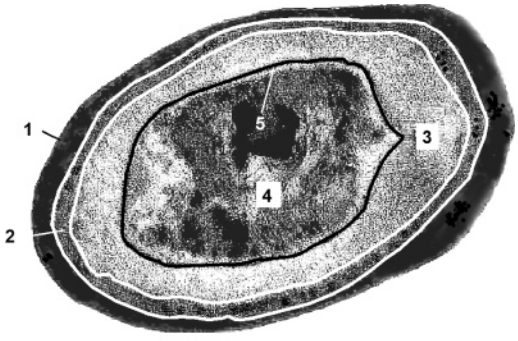

Figure 12. Contours of *B. subtilis* spore compartments adopted from the electron micrograph in ref 33. (1) The outer coat, (2) the inner coat, (3) the cortex, (4) the core, (5) the inner membrane. Bar = 500 nm.

Two types of ion exchange are existed in a multilayered structure like a spore. One is limited by diffusivity of ions within each layer ("film" diffusion), and other is limited by diffusivity of ions within the core ("particle" diffusion).[55] The time constant for the "particle" controlled diffusion is

$$\tau = \frac{r^2}{\pi^2 D_{\text{eff}}} \tag{17}$$

where r is the radius of a particle and D_{eff} is the effective diffusion coefficient of protons within the particle. Equation 17 was used for calculations of the effective diffusion coefficient within the spore core or the whole spore if the respective radii are known.

The time constant for the "film" controlled diffusion in the case of a single type of counter-ions (spores are diluted in pure water or in HCl solution and, no other counter-ions except hydrogen ions are present) is:

$$\tau = \frac{r\delta}{3D_{\text{eff}}} \tag{18}$$

where r is the radius of a spherical particle on which the film is deposited, δ is the thickness of the film, and D_{eff} is the effective diffusion coefficient of protons in the film. Equation 18 was used for calculations of the effective diffusion coefficient within spore layers (coats and cortex).

At this point, we estimated the thickness of the pre-surface layer (δ = 2.5−1.7 nm) by inputting into eq 18 the shortest time constants for the proton influx (0.09 s) and efflux (0.06 s) from Table 1, $D_{\text{eff}} = 5.8 \times 10^3$ nm^2/s from Table 2, and r = 629 nm from DLS measurements for the spore suspension in pure water with pH 6.1. Thus, the thickness of this layer, being on the order of 1−2 nm, is 300 to 600 times smaller than the radius of the spore and may be assigned to the so-called unstirred layer where the diffusion front is formed. At the lower initial pHs, the diffusion times for the proton influx across 2 nm distance were evaluated to be 2 to 4 orders of magnitude faster than the time resolution of our kinetic experiments. Therefore, the value of time constants present in each cell of Table 3 characterizes the diffusion through all layers located above the underlying one. For example, 4 s in the second cell from the

TABLE 3: Distribution of the Diffusion Times (in Seconds) through the Spore Structural Layers

$C_{sp} = 5.9 \times 10^{11}$ sp/L			$C_{sp} = 2.3 \times 10^{10}$ sp/L			
pH 6.10	pH 3.67	pH 2.23	pH 5.73	pH 3.62	pH 2.15	spore compartments diffused by protons
0.09						unstirred layer of ~2 nm thickness
	0.05					outer coat of ~69 nm thickness
0.4	0.2	0.11	0.3	0.25		
8	3	1	0.65	1		inner + outer coats of ~119 nm thickness
803	322	8	8.9	5.6	4.0	both coats + cortex of ~251 nm thickness
		252				coats + cortex + core = average radius of spore ~631 nm
2007	1164	693	175	250	3089	

bottom of the sixth column means that this value characterizes the proton diffusion from the spore surface up to the inner membrane surrounding the spore core. Importantly, the time constants in two last rows of Table 3 indicate that the effective diffusion coefficient for hydrogen ions within the spore core is significantly lower than the one within coats and cortex. It was commonly thought[56] that the coats and cortex are readily permeable to water and contain free water, whereas the core contains structured or bound water. However, a slower diffusivity of protons into the dormant spore core most likely results from a low permeability of the inner membrane which separates cortex and core. There is a vast pool of data[27,54] indicating the lipid immobility in the inner membrane of dormant spore. Since the inner membrane is not readily permeable to many compounds including small ions, it is definitely responsible for governing ion permeability into the "lockbox" of genetic information.

Our data in Table 3 show that the difference between proton diffusivities in the spore cortex and core significantly varies with the concentration of spores and initial concentration of protons. For example, in acidic medium (pH ~ 2), the diffusion times for the fluxes of protons across the distance including the core radius were hundreds times slower than those for the spore coats and cortex (cf. 693/8 ≈ 87, 3089/4 ≈ 772). The corresponding ratios of effective diffusion coefficients were estimated as the ratio of D_{eff}^{core} for the core (particle controlled diffusion by eq 17) and $D_{eff}^{coats + cortex}$ for the coats/cortex layer (film controlled diffusion by eq 18) $D_{eff}^{core}/D_{eff}^{coats + cortex} \approx 0.3r\tau_{coats + cortex}/\delta\tau_{core}$, to be 5.2×10^{-3} and 5.9×10^{-4}, respectively. Actually, this is a direct quantitative observation that the diffusion coefficients of protons differ for coats + cortex and core.

Conclusions

The data presented above is the first systematic study of (1) the equilibrium proton binding within *Bacillus subtilis* dormant spores and (2) the kinetics of pH equilibration in the external aqueous medium as a result of the proton transport in and out of the dormant spores. Similar to ionic hydrogels, the bacterial spores were characterized as ionic reservoirs with the average number of fixed charges (number of proton binding sites) on the polymer-like chains of internal matrix and the apparent binding constant specific to the particular type of the binding sites. Prior to this study, the type of ionizable groups, their exact number and distribution inside spores were unknown. The number of ionizable groups was estimated to be of $\sim 2 \times 10^{10}$ sites per spore. The apparent binding constant, K_{app}, was calculated from the slope of the Langmuir isotherm at low concentrations of protons to be of 5×10^4 M^{-1}. This value yields the apparent $pK_a \sim 4.7$, which allows us to assign the type of binding sites within the *B. subtilis* spores to carboxyl groups, COO^-, which molar concentration is $[n] \sim 35$ M indicating the extremely high proton capacity of each spore.

We showed that the concentrations of free hydrogen ions inside the spore can be up to 3 orders of magnitude higher than that outside the spore, whereas the concentrations of co-ions (chloride ions) were reversal on both sides of a spore surface. In the practical point of view, regulation of the spore internal pH may be the way of its metabolic dormancy control, since the internal pH may be a contributing factor to enzymatic activity within the dormant spore.[24,25]

Exploiting the concept of ionic reservoir for the dormant spores, we realize that the physical dimension of a spore is a result of a balance between the ion concentration difference and the mechanical elasticity of each spore structural layer. In this paper, we did not take into account the volume change because boundary conditions and density changes for spore multilayered matrix makes the equations for equilibrium binding and diffusion of ions extremely difficult to solve. However, we left this effect for the further experimental study by dynamic light scattering.

In this paper, we have introduced a method of time-resolved micropotentiometry for probing the kinetics of proton uptake by dormant *Bacillus subtilis* spores. It was shown that the plurality of steps comprising the uptake of protons may be attributed to the multilayered coats−cortex−inner membrane−core structure of the spores. The important conclusion derived from the time constants systematically presented for the spore structural layers is that the process of proton diffusion is not the same in coats + cortex and core matrices. The effective diffusion coefficient for hydrogen ions within the spore core can be significantly lower than the one within coats and cortex. The finding that the difference between proton diffusivities in the spore cortex and the spore core depends on the concentration of spores and initial concentration of protons is striking, since it may have a physiological importance as a physicochemical precursor of spore's quorum sensing mechanism.

Acknowledgment. This work was financially supported in part by Pace University (Dyson College of Art and Sciences, Summer Research Grant, Scholarly Research Fund, and Forensic Science Program). Acknowledgment is made to the Donors of the American Chemical Society/Petroleum Research Fund for partial support of this research (PRF Grant 44161-GB5). Our thanks go to Professor Kalle Levon (Polytechnic University, New York) for the gift of spores.

References and Notes

(1) Ricka, J.; Tanaka, T. *Macromolecules* **1984**, *17*, 2916.
(2) Fernandez-Nieves, A.; Fernandez-Barbero, A.; Vincent, B.; de las Nieves, F. J. *Macromolecules* **2000**, *33*, 2114.
(3) Shibayama, M.; Ikkai, F.; Inamoto, S.; Nomura, S.; Han, C. C. *J. Chem. Phys.* **1996**, *105*, 4358.
(4) Eichenbaum, G. M.; Kiser, P. F.; Simon, S. A.; Needham, D. *Macromolecules* **1998**, *31*, 5084.

(5) Suzuki, H.; Wang, B.; Yoshida, R.; Kokufuta, E. *Langmuir* **1999**, *15*, 4283.
(6) Khokhlov, A. R.; Kramarenko, Yu, E. *Macromolecules* **1996**, *29*, 681.
(7) Philippova, O. E.; Hourdet, D.; Audebert, R.; Khokhlov, A. R. *Macromolecules* **1997**, *30*, 8278.
(8) Saunders, B. R.; Crowther, H. M.; Vincent, B. *Macromolecules* **1997**, *30*, 482.
(9) De, S. K.; Aluru, N. R.; Johnson, B.; Crone, W. C.; Beebe, D. J.; Moore, J. *J. Microelectromech. Sys.* **2002**, *11*, 544.
(10) Halozan, D.; Dejugnat, C.; Brumen, M.; Sukhorukov, G. B. *J. Chem. Inf. Model.* **2005**, *43*, 1589.
(11) English, A. E.; Mafe, S.; Manzanares, J. A.; Yu, X.; Grosberg, A. Yu.; Tanaka, T. *J. Chem. Phys.* **1996**, *104*, 8713.
(12) Kazakov, S.; Kaholek, M.; Ji, T.; Turnbough, C. L., Jr.; Levon, K. *Chem. Commun.* **2004**, 430.
(13) Foster, S. J.; Johnstone, K. *Regulation of Prokaryotic Development;* Smith, I., Slepecky, R. A., Setlow, P., Eds.; Washington, DC: American Society for Microbiology, 1989; Chapter 4, pp 89−108.
(14) Ellar, D.J. *28th Symposium of the SGM*; Stanier, R. Y., Rogers, H. J., Ward, J. B., Eds.; Cambridge: CUP, 1978; pp 295−325.
(15) Gould, G. W. *J. Appl. Bact.* **1970**, *33*, 34.
(16) Gould, G. W. *J. Appl. Microbiol.* **2006**, *101*, 507.
(17) Moir, A. *J. Appl. Microbiol.* **2006**, *101*, 526.
(18) Stewart, G. S. A. B.; Johnstone, K.; Hagelberg., E.; Ellar, D. J. *Biochem. J.* **1981**, *198*, 101.
(19) Setlow, P. *The Bacterial Spore Volume 2*; Gould, G. W., Hurst, A., Eds.; Academic Press: London, 1983; p 211.
(20) Foerster, H. F. *Arch. Microbiol.* **1985**, *142*, 185.
(21) Strange, R. E.; Hunter, R. E. In *The Bacterial Spore*; Gould, G. W., Hurst, A., Eds.; London: Academic Press, Inc., 1969; p 445.
(22) Janoff, A. S. R.; Coughlin, T.; Racine, F. M.; McGroarty, E. J.; Vary, J. C. *Biochem. Biophys. Res. Commun.* **1979**, *89*, 569.
(23) Johnstone, K.; Stewart, G. S. A. B.; Scott, I. R.; Ellar, D. J. *Biochem. J.* **1991**, *208*, 407−411.
(24) Setlow, B.; Setlow, P. *PNAS* ***1980***, 77, 2474.
(25) Swerdlow, R. M.; Setlow, B.; Setlow, P. *J. Bacteriol.* **1981**, *148*, 20.
(26) Makino, S.; Moriyama, R. *Med. Sci. Monit.* **2002**, *8*, RA119−127.
(27) Cowan, A. E.; Olivastro, E. M.; Koppel, D. E.; Loshon, C. A.; Setlow, B.; Setlow, P. *PNAS* **2004**, *101*, 7733.
(28) Gould, G. W. *The Bacterial Spore 2*, pp 173−209. Edited by Gould, G.W. and Hurst, A. London: Academic Press, 1983.
(29) Warth, A. D.; Strominger, J. L. *Biochemistry* **1972**, *11*, 1389.
(30) Popham, D. L.; Setlow, P. *J. Bacteriol.* **1993**, *175*, 2767.
(31) (34) Lewis, J. C.; Snell, N. S.; Burr, H. K. *Science* **1960**, *132*, 544.
(32) Black, S. H.; Gerhardt, P. *J. Bacterial.* **1962**, *83*, 967.
(33) Driks, A. *Microbiol. Mol. Biol. Rev.* **1999**, *63*, 1.
(34) Kozuka, S.; Yasuda, Y.; Tochikubo, K. *J. Bacteriol*. **1985**, *162*, 1250.
(35) Murrell, W. G. *The Bacterial Spore*; Gould, G. W., Hurst, A., Eds.; Academic Press: London, 1980; pp 215−273.
(36) Lenz, G.; Gilvarg, C. *J. Bacteriol.* **1973**, *114*, 455.
(37) Gould, G. W. *The Bacterial Spore;* Gould, G. W., Hurst, A., Eds.; Academic Press: New York, 1969; pp 397−444..
(38) Tipper, D. J.; Gauthier, J. J. *Spores V*; Halvorson, H. O., Hanson, R., Campbell, L. L., Eds.; Amer. Soc. Microbiol., 1972; pp 3−12.
(39) Black, S. H.; Gerhardt, P. *J. Bacteriol.* **1962**, *83*, 960.
(40) Marshall, B. J.; Murrell, W. G. *J. Appl. Bacteriol.* **1970**, *33*, 103.
(41) Carstensen, E. L.; Marquis, R. E.; Gerhardt, P. *J. Bacteriol.* **1971**, 107, 106.
(42) Carstensen, E. L.; Marquis, R. E.; Child, S. Z.; Bender, G. R. *J. Bacteriol.* **1979**, *140*, 917.
(43) Kazakov, S.; Kaholek, M.; Gazaryan, I.; Krasnikov, B.; Miller, K.; Levon, K. *J. Phys. Chem. B* **2006**, *110*, 15107.
(44) Harwood, C. R.; Cutting, S. M. *Molecular Biological Methods for Bacillus;* J. Wiley & Sons: New York, 1990.
(45) Berne, B. J.; Pecora, R. *Dynamic light scattering with applications to chemistry, biology and physics*; Willey-Interscience: New York, 1976.
(46) Kazakov, S. V.; Galaev, I. Y.; Mattiasson, B. *Jnt. J. Thermophys.* **2002**, *23*, 161.
(47) Helfferich, F. *Ion Exchange;* McGraw: New York, 1962.
(48) Atkins, P. *Physical Chemistry*, 6th ed.; W. H. Freeman and Co.: New York, 1999.
(49) Brannon-Peppas, L.; Peppas, N. A. *Polym. Bull.* **1988**, *20*, 285.
(50) *CRC Handbook of Chemistry and Physics*, 71st ed.; Lide, D., Ed.; CRC Press: Boca Raton, FL, 1990.
(51) Cantor, C. R.; Schimmel, P. R. *Biophysical Chemistry, Part 3: The Behavior of Biological Macromolecules*; W. H. Freeman and Co.: San Francisco, 1980.
(52) Grimshaw, P. E.; Nussbaum, J. H.; Grodzinsky, A. J. *J. Chem. Phys.* **1990**, *93*, 4462.
(53) Narita, T.; Gong, J. P.; Osada, Y. *J. Phys. Chem.* **1998**, *102*, 4566.
(54) Nussbaum, J. H.; Grodzinsky, A. J. *J. Membr. Sci.* **1981**, *8*, 193.
(55) Marszalek, P. E.; Farell, B.; Vardugo, P.; Fernandez, J. M. *Biophys. J.* **1997**, *73*, 1169.
(56) Gould, G. W. *J. Appl. Bacteriol.* **1972**, *42*, 297.